Electric Field-Driven Spatial Information Capture of Dissipative Biocondensate States

Neetu, Aman Saini, Rishi Ram Mahato, Priyanka, Subhabrata Maiti*[,a]

[a] Department of Chemical Sciences, Indian Institute of Science Education and Research (IISER) Mohali, Knowledge City, Manauli 140306, India

*Email: smaiti@iisermohali.ac.in

Abstract

The theory behind origin of life to Darwinian evolution considers emergence of dissipative structures driven by the flow of energy across all length scales. To this end, developing and deeper understanding of non-equilibrium self-assembly processes under continuous supply of energy is a demanding matter, both in fundamental and application (for e.g. developing dynamic materials) viewpoint. Herein, we demonstrate transient self-assembly of a DNA-histone condensate where trypsin (already present in the system) hydrolyse histone resulting disassembly. As the process is short-lived, the information of intermediate states between complete assembly and disassembly remains uncaptured in absence of any external energy. We show that performing the process under electric field of varying strength results fractionation of myriad of short-lived states which appears as band in different zone. Deconvolution and capturing of many hidden self-assembling species of similar components but of different compositions which otherwise never be formed in absence of electric energy, will be of immense importance in applied non-equilibrium thermodynamics.

Graphical Abstract:

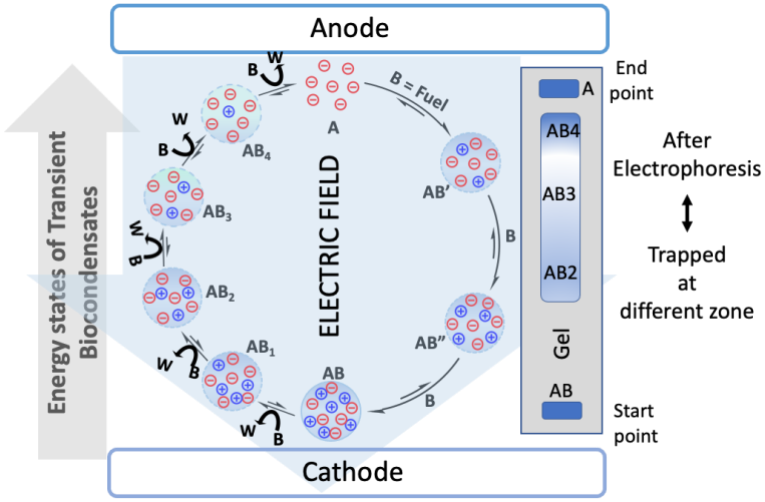

Dissipative spatial structures or patterns form under non-equilibrium conditions when chemical reactions or self-assembly processes are driven far from equilibrium by influx of energy or matter.[1,2] Therefore, one of the prerequisites to achieve dissipative pattern is the breakdown of kinetic symmetry of a chemical process by the appropriate amount of energy influx as kinetics play most important role in far from equilibrium regime.[3,4] Reaction-diffusion driven system like Turing pattern (TP) or Liesegang pattern (LP) are known examples of this kind of structures/patterns. Importantly, both TP and LP have relevance in understanding biological pattern (for example, morphogenesis, skin stripes to fingerprint) to geochemical patterns (for example - oscillatory zoning during magma crystallization, planetary orbit system).[5-6] Recently, chemists also generated LP in several synthetic systems based on nanoparticle assembly in hydrogel matrix mediated by pH gradient or modulating the surface charge of interacting species to achieve stationary inhomogeneous but controlled distribution of particle deposition in space.[7-10]

In this context, spatial transport can also be governed by applying energy in addition to diffusion.[11] Therefore, many metastable or transiently stable state in a chemical process can be transported by applying energy and thus information can be stored in a different zone. This can be, of relevance, in getting multiple diversified off-spring from one common ancestor relevant to Darwinian evolutionary aspect.[12] On the other hand, in an equilibrium system (without input of external energy) stabilization of such short-lived states which may be of high energy as well as functionally organized seems improbable. Overall, in the context of origin of life and evolutionary scenario, this fact of stabilizing far from equilibrium intermediate forms is highly recognized.[13,14] In this manuscript, we explored by applying electric energy of different amplitude, how information of a multiple short-lived states pertinent to a transient assembly process can be trapped in different zone.

Many recent literature reports demonstrate chemical fuels or stimuli driven process via non-covalent interaction with the self-organizing unit (like – surfactant, nanoparticle etc.) can create transient assembled systems under dissipative condition.[15-28] Here, dissipative condition suggests simultaneous degradation of the fuel or stimuli by another process (for e.g. enzymatic degradation, conformational switching) in such a way that the interactivity with building block ceases, resulting transient assembly.[29] The pre-programmable and regenerative nature of this process find application in designing complex reaction network, reconfigurable materials with life-like properties.[26,29] However, still now, the system has been considered as a two different energy state system, where assembly process is fast, whereas disassembly process is slow. One can easily think of many multiple intermediate states and each can have different property. In fact, trapping these states by experimental means will help us to achieve simultaneous collection of many self-organized species (same components but compositionally different) which cannot be possible by any other way. Previously, we theoretically deconvoluted the intermediate species of a system which is under dissipative condition where we found compositions of each species are also changing non-linearly.[30] However, realization of this by experimental process has not been carried out until now

although it has enormous fundamental and applicative importance as discussed in the preceding paragraphs. To perceive the above-mentioned facts experimentally, we use histone as chemical fuel which results assembly of DNA to generate chromatin-like condensates (coacervate in nature) (Figure 1).[31-32] However, when trypsin is pre-mixed in DNA, then addition of histone results transient formation of coacervates (where DNA-histone binding is fast and trypsin-mediated histone dissociation is relatively slow).[33] However, when this dynamic process is carried out in presence of electric field, then multiple states during downhill process can get accumulated in different zone. Additionally, with increasing electric field, the intermediate states with faster dissipation process can also be trapped. The details results showing transient coacervate formation (including enthalpic and entropic parameters) in static and under electric field are discussed below.

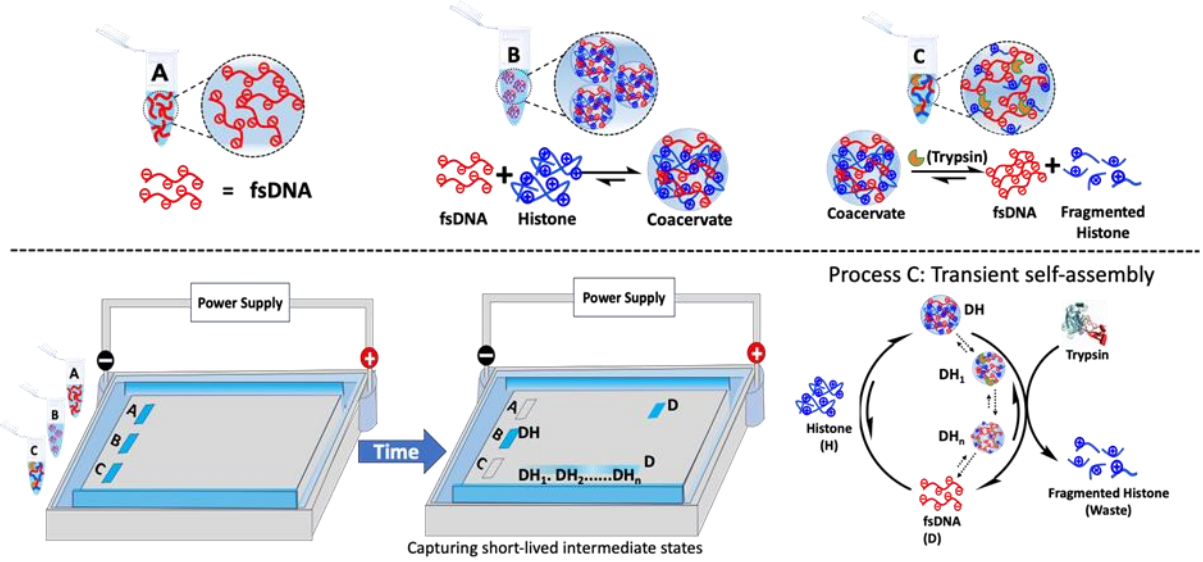

Figure 1. Schematic representation of the system involved including electrophoresis experiment in agarose gel bed. Here we show intermediate short-lived states mentioned as DH_1 to DH_n can be trapped during gel electrophoresis when system is under non-equilibrium condition.

At first, we checked the formation kinetics of DNA-histone coacervate in absence and presence of trypsin. Upon addition of histone in a transparent solution containing DNA in HEPES buffer pH = 8.0 , the solution becomes turbid due to formation of 1-2 μm sized DNA-histone condensates (Figure S1, SI). Turbidity kinetics has been checked via UV-vis spectroscopy at 500 nm and the condensate remains stable at a fixed A500 value of 0.35 for more than 90 min and it takes around 20 min to reach the thermodynamically stable condition. The dimension of the condensates was checked by dynamic light scattering (DLS) and optical microscopic images (Figure S5, S6, S10, SI). Importantly, scattering by the condensates was also checked by count rate analysis while performing DLS measurement and count rate was increased from 2-3 kCPS to 300 ± 50 kCPS, after addition of histone in DNA solution.

Now, our aim was to conduct DNA-histone formation under dissipative condition and for that we used trypsin enzyme premixed in DNA solution. In this case, after adding histone in the system, we observed transient formation of condensates.[31-32] Here, trypsin acts as a protease which fragments the histone, resulting dissociation of the condensate.[33] We showed the lifetime of the condensate can be manipulated by changing the concentration of histone and trypsin. With increasing histone concentration from 5 to 50 μM by keeping DNA (2 μM) and trypsin (200 nM) fixed, the half-life of the condensate can be increased from 2 to 25 min (Figure 2a, Figure S3, SI). On the otherhand, keeping DNA (2 μM) and histone (5 μM) fixed, increasing trypsin from 20 nM to 200 nM the half-life of the condensate can again be decreased from 25 to 5 min (Figure 2b, Figure S4, SI).

Next, we measured the change in zeta potential of DNA upon addition of different amount of histone. We observed with increasing histone concentration, zeta potential increased in a sigmoidal manner and -ve zeta value of DNA (5 μM) changed to +ve zeta potential upon titration of histone from 3 to 18 μM. Interestingly, the value was -10 mV until addition of 8 μM histone, which jumps to +9 mV, in presence of 9 μM histone (Figure 2c, Figure. 13, SI). Next, we made a condensate using 5 μM DNA and 12.5 μM of histone and measured zeta potential up to almost 1 hr and found the zeta potential remains stable at +20 mV (Figure 2d). Interestingly, in presence of increasing concentration of trypsin (10-100 nM), the zeta value started to decrease at a faster rate (Figure 2d, S14, SI). Interestingly, even at a very low concentration of trypsin the decrease from +ve zeta value to neutral or -ve value was almost instantaneous, suggesting little amount of trypsin is enough to perturb the inherent stability or charge-balance state of the condensate. We also performed count rate decrease kinetics over time at different amount of trypsin concentration and also found it decreased sharply with increasing trypsin amount (Figure 3e). Unfortunately, we were not able to find out the temporal decrease in hydrodynamic diameter (D_h) of the condensates as it resulted too polydisperse data during dissociation by trypsin. Additionally, optical microscopic images over time clearly indicates the disappearance of spherical DNA-histone condensates in presence of trypsin over time (Figure 2f, S7-9, 11, 12, SI).

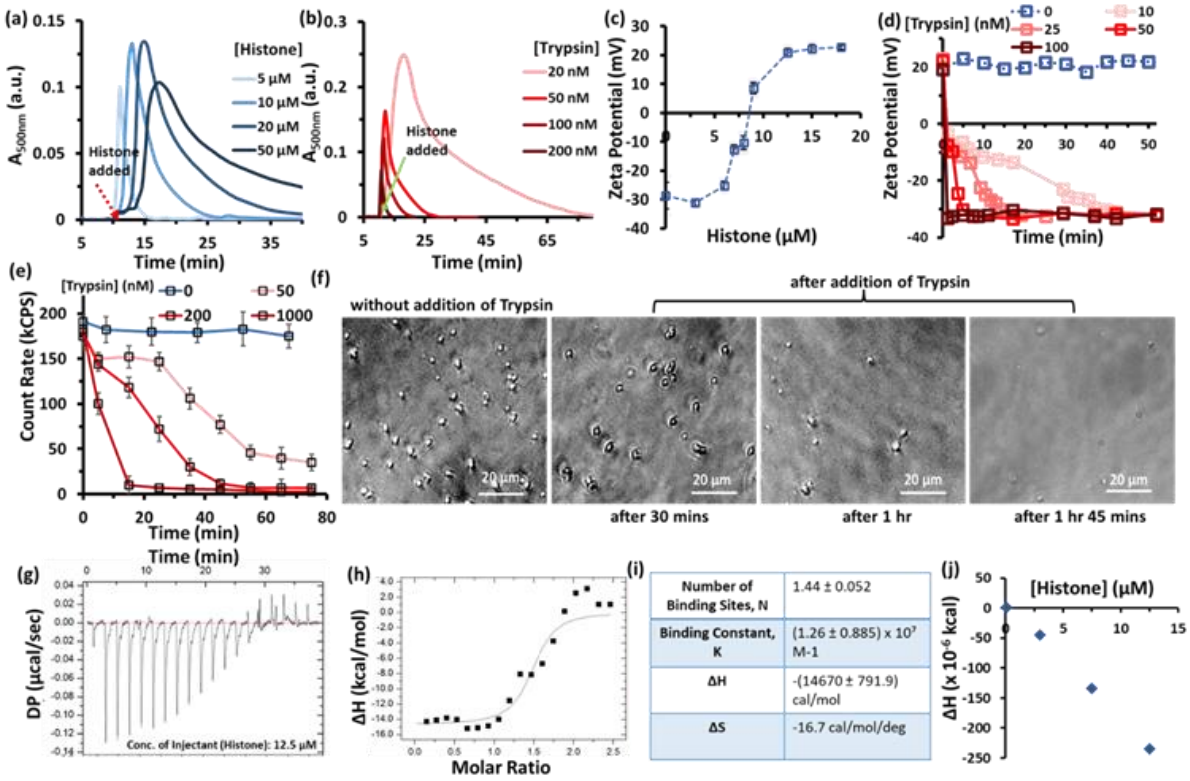

Figure 2. UV-Vis absorbance (A_{500}) with time after addition of Histone at 10 min due to the transient formation of: (a) DNA (2 µM) and Histone (different concentrations, 5-50 µM) coacervates when Trypsin (200 nM) is premixed with DNA, (b) DNA (2 µM) and Histone (5 µM) coacervates with time when different concentrations of Trypsin (20-200 nM) are pre-mixed with DNA. Change in zeta potential of: (c) DNA (5 µM) after addition of varying concentrations of Histone (3-18 µM), (d) DNA (5 µM) and Histone (12.5 µM) coacervates with time after addition of different concentrations of Trypsin (10-100 nM), (e) Change in count rate of DNA (5 µM) and Histone (12.5 µM) coacervates with time after addition of different concentrations of Trypsin (50-1000 nM), (f) Brightfield microscopic images of DNA (5 µM) and Histone (12.5 µM) coacervates after addition of 50 nM Trypsin. (g) and (h) Isothermal Titration Calorimetry (ITC) isotherm of DNA (5 µM) with Histone (12.5 µM) using multi-injection method. (i) Thermodynamic parameters of DNA (5 µM) and Histone (12.5 µM) Binding. (j) Enthalpy change (ΔH) plot of DNA (5 µM) with different Histone concentration (12.5 µM) using single-injection method. Experimental conditions: [HEPES] = 5 mM; pH 8.0, *T* = 25 °C.

Next, we performed isothermal titration calorimetry (ITC) measurement to find out the exact thermodynamic parameter (enthalpy, entropy of the condensates) which by itself has its own significance as DNA-histone condensates are actually chromatin. The energy needed to coiling of DNA inside the nucleus is provided by histone. Herein, we found in our system, the binding is highly exothermic, enthalpically favorable with a ΔH value of $-(14.6 \pm 0.7)$ kcal/mol and entropically slightly unfavorable having ΔS of -16.7 cal/mol/deg (Figure 2g-i). The binding constant is also high with a K value of $(1.26 \pm 0.8) \times 10^7$ M^{-1}. We also performed single injection experiment to find the amount of total amount of heat generated due to addition of different amount of histone (0.1 - 12.5 µM) at fixed DNA concentration (Figure 2j). We observed it almost followed a linear trend where energy release is proportional to the amount of histone

added in the system. This experiment also indicates one important fact that in principle, during degradation of histone by trypsin, condensate with different energy value can get produced.

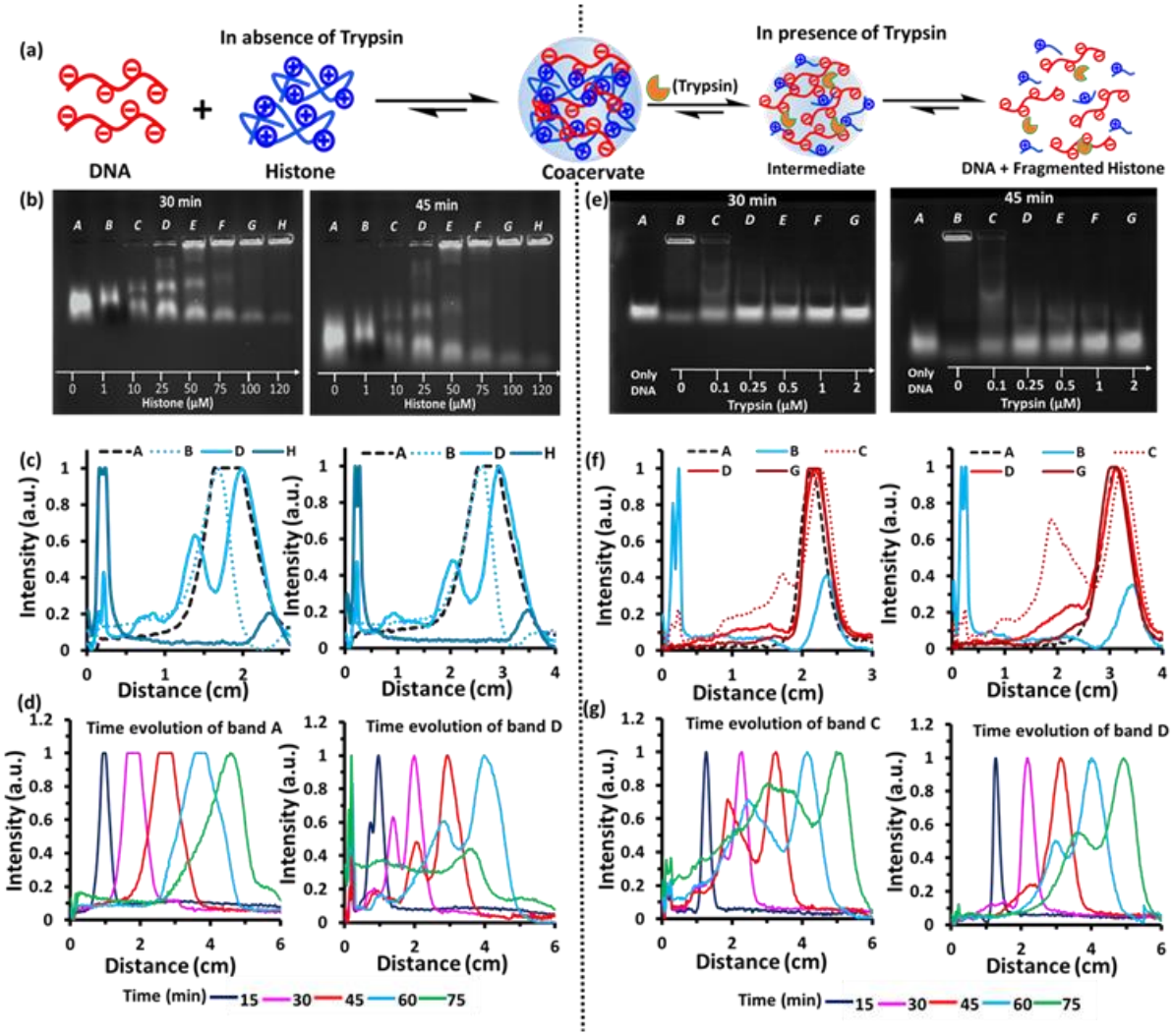

Figure 3. (a) Schematic representation of formation of DNA and Histone coacervates and dissociation after addition of Trypsin (b) 1.5% Agarose gel images after 30 mins and 45 mins of electrophoresis at 75 V having samples: (A) 100 μM DNA, (B) 100 μM DNA with 1 μM Histone, (C) 100 μM DNA with 10 μM Histone, (D) 100 μM DNA with 25 μM Histone, (E) 100 μM DNA with 50 μM Histone, (F) 100 μM DNA with 75 μM Histone, (G) 100 μM DNA with 100 μM Histone, (H) 100 μM DNA with 120 μM Histone. (c) Intensity vs distance plots of specific bands (A,B,D,H) of respective gel images in (b). (d) Time evolution of bands A and D of respective gel images shown in (b). (e) 1.5% Agarose gel images after 30 mins and 45 mins of electrophoresis at 75 V having samples: (A) 100 μM DNA, (B) 100 μM DNA and 120 μM Histone, (C) 100 μM DNA and 120 μM Histone with 100 nM Trypsin, (D) 100 μM DNA and 120 μM Histone with 250 nM Trypsin, (E) 100 μM DNA and 120 μM Histone with 500 nM Trypsin, (F) 100 μM DNA and 120 μM Histone with 1 μM Trypsin, (G) 100 μM DNA and 120 μM Histone with 2 μM Trypsin. (f) Intensity vs distance plots of specific bands (A,B,C,D,G) of respective gel images in (e). (g) Time evolution of bands C and D of respective gel images shown in (e). Experimental conditions: [HEPES] = 5 mM, pH 8.0, Running buffer: 1x TB buffer, T = 25 °C.

Next, we were curious to investigate the effect of external energy in the transient self-assembled biocondensate system under dissipative condition as discussed in the preceding paragraph. It is important to note electric field based molecular motor and achieving high energy state in a molecular system mainly having mechanical bond based supramolecular assembly system has been reported in recent literature.[34-39] In fact, one of the recent study indicated the entropy stored in that type of system.[37] However, none of the cases, effect of further complexity by application of external electric field in transient self-assembly process as discussed here, has been reported. We argued that it could be highly beneficial as it can deconvolute many short-lived states of different amount of energy stored can be trapped. For this, we used agarose gel electrophoresis as mentioned in Figure 1 and SI. At first, we performed experiment with only DNA and histone without adding any trypsin at 1.5 % agarose gel and 75 V fixed electric voltage and also measured the phoresis of DNA or DNA-histone condensates at different time interval (15-75 min) (Figure 3). We observe the position of the DNA species by illumination of intercalator ethidium bromide (EB) fluorescence under gel doc (Figure S17, SI). As usual DNA (negative charged species) moved towards cathode (line A in the gel) and with increasing concentration of histone, multiple bands started to appear with lesser cumulative phoretic effect over time (Figure 3c,d, S15, SI). For instance, at high histone concentration (0.12 mM), we observed no free DNA and no phoresis as all the condensate remain in the well even after applying voltage for 75 min. However, at intermediate concentration of histone we observed multiple bands corresponding to unbound, partially bound and fully bound DNA-histone condensates. Importantly, here phoresis depends both on the charge and dimension of the condensates and inevitably, only the negatively charged DNA-histone complex will move towards cathode.

Next, we performed the similar process in presence of different concentration of trypsin (0-2 μM), but at fixed concentration of histone (120 μM) where no phoresis effect was observed. Importantly, as observed in Figure 2, introduction of trypsin results transiently formed condensates and the transiency time can be dictated by the amount of trypsin. Interestingly, upon applying 0.1 μM trypsin, we observed a continuous band, alongwith free DNA (Figure 3e-g, Figure S16, SI). With increasing trypsin concentration, band trailing decreases and accumulation of free DNA increased. The most important fact here that band appearance is more continuous than observed in absence of trypsin by comparing data of Figure 3c and 3f, line C. It implied application of electric field can capture many more states at spatially different location when the system is under non-equilibrium condition. It is important to note that we observe only negatively charged states which actually have low histone composition and arguably, the dimension of those complex will also be smaller to move through gel.

We also checked the effect of gel porosity by using agarose gel matrix of lower (0.75%) and higher (3%) weight percentage (Figure S22, S23, SI). At 0.75% gel, we observed clear appearance of band at different position lower to DNA (corresponding to DNA-histone complex of different composition) and their relative with free DNA decreased with increasing concentration of trypsin. With lower concentration of trypsin (0.1 μM) we also observed

similar type of extended trailing at a lower extent of phoretic drift. At higher gel concentration (3%), the band of only DNA is relatively less sharper, however, the trend in data is almost similar. Overall, this study clearly indicated trapping of diverse but distinctively patterned composition of biocondensate under non-equilibrium condition by applying electrical field, which can not be achieved in other case.

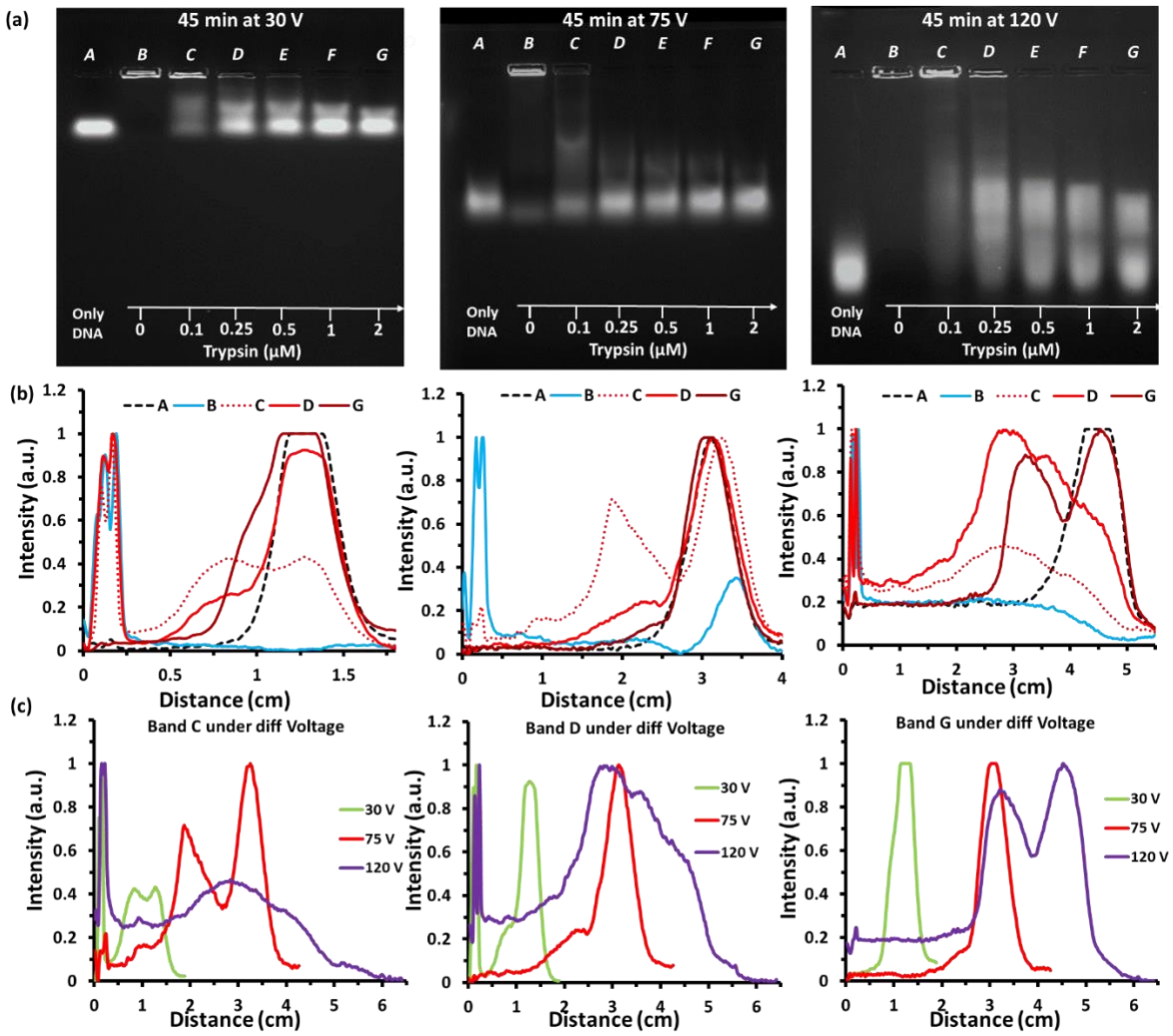

Figure 4. (a) 1.5% Agarose gel images after 45 mins of electrophoresis at different voltages (30 V, 75 V, 120 V) having samples: (A) 100 μM DNA, (B) 100 μM DNA and 120 μM Histone, (C) 100 μM DNA and 120 μM Histone with 100 nM Trypsin, (D) 100 μM DNA and 120 μM Histone with 250 nM Trypsin, (E) 100 μM DNA and 120 μM Histone with 500 nM Trypsin, (F) 100 μM DNA and 120 μM Histone with 1 μM Trypsin, (G) 100 μM DNA and 120 μM Histone with 2 μM Trypsin. (b) Intensity vs distance plots of specific bands (A,B,C,D,G) of respective gel images in (a). (c) Comparison of Intensity distribution of band C, D and G due to electrophoresis at 30 V, 75 V and 120 V. Experimental conditions: [HEPES] = 5 mM, pH 8.0, Running buffer: 1x TB buffer, T = 25 °C.

Finally, we explored the effect of electric field of varying strength in patterning DNA or DNA-histone complex in the gel. For this, we used one 30 V and other 120 V electric field and followed the composition of band structure (Figure 4, Figure S24, SI)). At 30 V, the electrophoretic drift is low and separation is distinct. However, at high voltage 120 V, the

separation became more distinctive. In fact, here we get a band trailing even at higher dissipation strength i.e. higher trypsin concentration as seen in D line. However, in lower voltage (75 V) we observed trailing at C line, with 0.1 μM of trypsin concentration (Figure 4c). It is worthy to mention, we reuse figure 3e (75 V, 45 min data) here for clear comparison of different voltage data. This experiment implies by incorporating high voltage of electric field, the even more short-lived biocondenstae states with rather dissipated at a faster rate, can also be trapped in different zone.

Overall, we have demonstrated capturing of short-lived states of different energy level in dissipative process via application of external energy which is of importance in the current context of non-equilibrium self-assembly and energy ratchet process involved therein.[3,4,40,41] Notably, through ITC experiment we quantified the amount of energy in biocondensate or DNA-histone complex with fixed DNA and varying histone composition. Additionally, we also demonstrated the patterning of DNA either in complex or free form is substantially different in dissipating condition. To the best of our knowledge this is the first non-equilibrium system where external energy in the form of electric voltage applied in a fuel-driven transient self-assembly process which in turn, actually results formation of dissipative pattern in gel. In fact, many more possible states can get trapped, depending on the amount of applied electric field and strength of dissipation. Therefore, this work can be of importance in applied non-equilibrium thermodynamics. One can also envision the importance of spatiotemporally controlled DNA-patterning obtained by applying electric field will also be potentially important not only in the area of dissipative DNA nanotechnology, but also be applicable in designing of different kind of spatiotemporally distinct dissipative synthetic system. [42-52]

Acknowledgements

S. M. acknowledges the financial support of the of Science and Engineering Research Board (SERB) (File No. CRG/2022/002345). Neetu, R.R.M. and Priyanka acknowledge IISER Mohali for doctoral research grant.

References:

[1] Prigogine, *Int. J. Quantum Chem.* **2009**, *9*, 443–456.
[2] A. Goldbeter, *Philos. Trans. A Math. Phys. Eng. Sci.* **2018**, *376*, 20170376.
[3] R. D. Astumian, *Nat. Commun.* **2019**, *10*, 3837.
[4] I. Aprahamian, S. M. Goldup, *J. Am. Chem. Soc.* **2023**, *145*, 14169–14183.
[5] H. Nabika, M. Itatani, I. Lagzi, *Langmuir* **2020**, *36*, 481–497.
[6] K. Asakura, R. Konishi, T. Nakatani, T. Nakano, M. Kamata, *J. Phys. Chem. B* **2011**, *115*, 3959–3963.
[7] B. Dúzs, P. De Kepper, I. Szalai, *ACS Omega* **2019**, *4*, 3213–3219.
[8] B. Dúzs, G. Holló, H. Kitahata, E. Ginder, N. J. Suematsu, I. Lagzi, I. Szalai, *Commun. Chem.* **2023**, *6*, 3.
[9] I. Lagzi, B. Kowalczyk, B. A. Grzybowski, *J. Am. Chem. Soc.* **2010**, *132*, 58–60.
[10] M. Itatani, Q. Fang, I. Lagzi, H. Nabika, *Phys. Chem. Chem. Phys.* **2022**, *24*, 2088–2094.
[11] A. Scagliarini, I. Pagonabarraga, *Soft Matter* **2020**, *16*, 8893–8903.

[12] S. Otto, *Acc. Chem. Res.* **2022**, *55*, 145–155.
[13] J. L. England, *Biophys. Rev. (Melville)* **2022**, *3*, 041303.
[14] P. Ván, *Philos. Trans. A Math. Phys. Eng. Sci.* **2020**, *378*, 20200066.
[15] L. Heinen, T. Heuser, A. Steinschulte, A. Walther, *Nano Lett.* **2017**, *17*, 4989–4995.
[16] R. K. Grötsch, C. Wanzke, M. Speckbacher, A. Angı, B. Rieger, J. Boekhoven, *J. Am. Chem. Soc.* **2019**, *141*, 9872–9878.
[17] A. M. Green, C. K. Ofosu, J. Kang, E. V. Anslyn, T. M. Truskett, D. J. Milliron, *Nano Lett.* **2022**, *22*, 1457–1466.
[18] M. Weißenfels, J. Gemen, R. Klajn, *Chem* **2021**, *7*, 23–37.
[19] N. Singh, B. Lainer, G. J. M. Formon, S. De Piccoli, T. M. Hermans, *J. Am. Chem. Soc.* **2020**, *142*, 4083–4087.
[20] B. Rieß, R. K. Grötsch, J. Boekhoven, *Chem* **2020**, *6*, 552–578.
[21] S. Maiti, I. Fortunati, C. Ferrante, P. Scrimin, L. J. Prins, *Nat. Chem.* **2016**, *8*, 725–731.
[22] J. L.-Y. Chen, S. Maiti, I. Fortunati, C. Ferrante, L. J. Prins, *Chem.- Eur. J.* **2017**, *23*, 11549–11559.
[23] I. Maity, N. Wagner, R. Mukherjee, D. Dev, E. Peacock-Lopez, R. Cohen-Luria, G. Ashkenasy, *Nat. Commun.* **2019**, *10*, 4636.
[24] E. Te Brinke, J. Groen, A. Herrmann, H. A. Heus, G. Rivas, E. Spruijt, W. T. S. Huck, *Nat. Nanotechnol.* **2018**, *13*, 849–855.
[25] A. Mishra, S. Dhiman, S. J. George, *Angew. Chem.* **2021**, *133*, 2772–2788.
[26] A. Sharko, D. Livitz, S. De Piccoli, K. J. M. Bishop, T. M. Hermans, *Chem. Rev.* **2022**, *122*, 11759–11777.
[27] R. R. Mahato, E. Shandilya, B. Dasgupta, S. Maiti, *ACS Catal.* **2021**, *11*, 8504–8509.
[28] Priyanka, E. Shandilya, S. K. Brar, R. R. Mahato, S. Maiti, *Chem. Sci.* **2021**, *13*, 274–282.
[29] F. Della Sala, S. Neri, S. Maiti, J. L.-Y. Chen, L. J. Prins, *Curr. Opin. Biotechnol.* **2017**, *46*, 27–33.
[30] E. Shandilya, S. Maiti, *ChemSystemsChem* **2020**, *2*, DOI 10.1002/syst.201900040.
[31] J. Bednar, R. A. Horowitz, S. A. Grigoryev, L. M. Carruthers, J. C. Hansen, A. J. Koster, C. L. Woodcock, *Proc. Natl. Acad. Sci.* **1998**, *95*, 14173–14178.
[32] R. D. Kornberg, *Science* **1974**, *184*, 868–871.
[33] H. Weintraub, F. Van Lente, *Proc. Natl. Acad. Sci.* **1974**, *71*, 4249–4253.
[34] L. Zhang, Y. Qiu, W.-G. Liu, H. Chen, D. Shen, B. Song, K. Cai, H. Wu, Y. Jiao, Y. Feng, J. S. W. Seale, C. Pezzato, J. Tian, Y. Tan, X.-Y. Chen, Q.-H. Guo, C. L. Stern, D. Philp, R. D. Astumian, W. A. Goddard 3rd, J. F. Stoddart, *Nature* **2023**, *613*, 280–286.
[35] C. Pezzato, M. T. Nguyen, C. Cheng, D. J. Kim, M. T. Otley, J. F. Stoddart, *Tetrahedron* **2017**, *73*, 4849–4857.
[36] G. Ragazzon, M. Malferrari, A. Arduini, A. Secchi, S. Rapino, S. Silvi, A. Credi, *Angew. Chem.* **2023**, *135*, DOI 10.1002/ange.202214265.
[37] S. Di Noja, M. Garrido, L. Gualandi, G. Ragazzon, *Chemistry* **2023**, *29*, DOI 10.1002/chem.202300295.
[38] G. Ragazzon, L. J. Prins, *Nat. Nanotechnol.* **2018**, *13*, 882–889.
[39] S. Corra, M. T. Bakić, J. Groppi, M. Baroncini, S. Silvi, E. Penocchio, M. Esposito, A. Credi, *Nat. Nanotechnol.* **2022**, *17*, 746–751.
[40] D. M. Busiello, S. Liang, F. Piazza, P. De Los Rios, *Commun. Chem.* **2021**, *4*, 16.
[41] T. Marchetti, D. Frezzato, L. Gabrielli, L. J. Prins, *Angew. Chem. Int. Ed* **2023**, DOI 10.1002/anie.202307530.
[42] Y. Vyborna, J.-C. Galas, A. Estevez-Torres, *J. Am. Chem. Soc.* **2021**, *143*, 20022–20026.
[43] Q. Liu, H. Li, B. Yu, Z. Meng, X. Zhang, J. Li, L. Zheng, *Adv. Funct. Mater.* **2022**, *32*, 2201196.
[44] Z. Li, J. Wang, I. Willner, *Adv. Funct. Mater.* **2022**, *32*, 2200799.
[45] E. Del Grosso, E. Franco, L. J. Prins, F. Ricci, *Nat. Chem.* **2022**, *14*, 600–613.
[46]J. Wang, Z. Li, Z. Zhou, Y. Ouyang, J. Zhang, X. Ma, H. Tian, I. Willner, *Chem. Sci.* **2021**, *12*, 11204–11212.
[47] E. Shandilya, S. Maiti, *ACS Nano* **2023**, *17*, 5108–5120.

[48] R. R. Mahato, Priyanka, E. Shandilya, S. Maiti, *Chem. Sci.* **2022**, *13*, 8557–8566.
[49] K. Das, L. Grabielli, L. J. prins, *Angew. Chem. Int. Ed* **2021**, *60*, 20120-20143.
[50] M. Kagan, D. Avnir, *Orig. Life* **1984**, *14*, 365–373.
[51] Z. Qin, Y. Liu, L. Zhang, J. Liu, X. Su, *ACS Nano* **2022**, *16*, 14274–14283.
[52] J. M. Grogan, N. M. Schneider, F. M. Ross, H. H. Bau, *Nano Lett.* **2014**, *14*, 359–364.